IEEE Access
Multidisciplinary ⋮ Rapid Review ⋮ Open Access Journal

Received 29 August 2022, accepted 13 September 2022, date of publication 19 September 2022,
date of current version 27 September 2022.

Digital Object Identifier 10.1109/ACCESS.2022.3207836

RESEARCH ARTICLE

Gait Identification Using Limb Joint Movement and Deep Machine Learning

LUKE K. TOPHAM[1], WASIQ KHAN[1], (Member, IEEE), DHIYA AL-JUMEILY[1], (Senior Member, IEEE), ATIF WARAICH[1], AND ABIR J. HUSSAIN[2], (Member, IEEE)

[1]School of Computer Science and Mathematics, Liverpool John Moores University, L3 3AF Liverpool, U.K.
[2]College of Engineering, University of Sharjah, Sharjah, United Arab Emirates

Corresponding author: Wasiq Khan (w.khan@ljmu.ac.uk)

This work involved human subjects or animals in its research. Approval of all ethical and experimental procedures and protocols was granted by the University Research Ethics Committee (UREC) of Liverpool John Moores University under Reference No. 21/CMP/004.

ABSTRACT Person identification is a key problem in the security domain and may be used to automatically identify criminals or missing persons. The traditional face matching approaches adopted by the police and security services across the world have recently been shown to produce a high rate of false positive identification. Alternatively, gait-based person identification has shown to be a convenient method particularly as it can be performed at a distance, without the cooperation of the subject, and is a biometric trait which cannot be easily disguised. In this work, we propose a gait-based person identification approach which uses limb joint motion data and deep machine learning models to identify the individuals. Distinct statistical features are identified and extracted from limb movement using a fixed width sliding window to train a Long Short-Term Memory model. The proposed solution outperforms the existing methods producing 98.87% accuracy when evaluated over unseen samples. In addition, we propose a simple two-stage filtering approach to increase the prediction accuracy up to 100% when identifying individuals from larger sequences of samples. This finding may improve the current solutions in controlled environments such as airports. In the future, this approach may help to overcome the problem of occlusion in gait-based identification, as unlike the existing works, it does not require information regarding the entire body. The study also presents a primary dataset comprising limb joint movement acquired from a diverse range of participants during casual walking captured through two digital goniometers.

INDEX TERMS Gait identification, limb joint motion analysis, gait recognition, deep learning for person identification, gait pattern recognition, IMU sensor data.

I. INTRODUCTION

Person identification is a key issue mainly within the security domain. The media has highlighted several cases where the concerned authorities (e.g. police force) have been using Face Matching Tools (FMT) which provided false positive rates up to 98% [1], [2], [3]. In these solutions, false positives incorrectly identify innocent members of the public as crime suspects. Real-time dynamic environments pose problems for FMT, for example, pose variation, lighting, facial expressions, image resolutions, makeup, and occlusion can cause identification failure [4]. Such reports suggest a clear need for an improved approach to automated person identification.

An alternative approach to FMT for person identification is provided by gait identification, whereby a person is identified by the manner of their walking. Gait analysis is considered to be a convenient approach to person identification as it can be performed at a distance, without the knowledge or cooperation of the subject, and it is a feature which cannot be easily disguised [5]. Such factors would be advantageous

The associate editor coordinating the review of this manuscript and approving it for publication was Dost Muhammad Khan.

in addressing problems such as crime suspect identification, and missing person identification.

Furthermore, computer vision-based approaches to gait identification provide the opportunity to obtain the aforementioned covert advantages of gait identification and have therefore gained significant attention. However, existing computer vision-based gait identification solutions are often affected by occlusion and clothing changes, this is partly due to the whole body approach where data is required for the entire body movement, which is not always available in real-world dynamic environments [6], [7]. Many of the existing sensor-based datasets encourage a whole body approach by capturing data using networks of sensors to capture full body movement, or via sensors attached to the trunk [8]. To the best of the authors' knowledge, none of the existing dataset contain movement data for multiple individual limbs or joints. Such a dataset would allow researchers to approach the problem of gait identification in situations where whole body information is not available, for example, when the body is partially occluded.

This work proposes a new gait-based person identification approach using movement data regarding multiple body-joints and machine/deep learning algorithms. Movement data is collected for the hip and shoulder joints using an Inertial Measurement Unit (IMU)-based digital goniometer device. Goniometers are commonly used by physiotherapists to measure the range-of-motion (*i.e.,* angle) of a body joint [9]. Digital goniometers commonly include IMU sensors containing accelerometers, gyroscopes, and magnetometers to measure movement [10].

To the best of the authors' knowledge, this is the first use of a body joint-based approach to gait-based person identification which may in the future offer the opportunity to decrease the impact of problems such as occlusion in computer vision-based gait identification. We present a novel primary dataset comprising 30 diverse participants. The dataset contains movement data from both arm and leg joints (*i.e.,* hip and shoulder joints) recorded during normal walking sequences via wearable IMU-based digital goniometers. Furthermore, we also present unique feature vectors generated by time-series analysis of the limb movement data from our acquired dataset. This helps explaining the distinct spatial and temporal gait information which can be used for robust person identification. Moreover, we describe a simple two-stage approach to filtering the gait identification predictions which may be applied to alternative solutions.

The remainder of this work is organized as follows. Section II presents an overview of the current works related to IMU-based gait identification. Section III presents the proposed methodology and experimental design. Section IV presents the detailed experimental methodology followed by the experimental results in Section V. Further discussions regardomg the results and findings are provided in Section VI. Finally, Section VII presents the conclusions and plans for future work.

TABLE 1. Related wearable sensor-based works.

Ref	Sensor Type	Sensor Placement	Model	Gait Task
[14]	Accelerometer	Trunk	KNN	Identification
[15]	IMU	Trunk	RCE	Analysis
[16]	IMU	Trunk	Hidden Markov	Analysis
[17]	Accelerometer	Trunk	LSTM	Identification
[18]	IMU	Wrist	CNN	Identification
[19]	IMU	Ankle	CNN / SVM	Identification
[20]	IMU	Trunk	GMM-UBM	Identification
[21]	IMU	Trunk	CNN	Identification
[22]	IMU	Ankle	RRS	Identification

II. RELATED WORK

For decades, psychologists have been able to demonstrate that people are able to recognise individuals based solely on the way that they walk [11], [12]. Early attempts at technological gait analysis included rule-based systems such as in [13], however, very little work on technological approaches to gait identification were reported before machine learning became prominent, after which, significant advances have been made.

Several existing works have explored machine learning approach to gait identification, as shown in Table 1. For instance, [14] used a clustering algorithm in combination with an accelerometer-based device to learn the users' gait pattern when they first begin to use the device. Then K-Nearest Neighbour (KNN) clustering is used to classify whether detected footsteps belong to a known and approved user of the device or not [14]. This approach is appropriate where it is necessary to confirm the access rights of a single person in a one-vs-all fashion (*e.g.,* to grant or refuse access to a device), however, it is not appropriate in its current form for problems where people must be identified from a known list of individuals (*i.e.,* multiple class classification). Despite this, an unsupervised approach has been demonstrated for gait analysis in [15] which makes use of Rapid Centroid Estimation (RCE) for clustering, and also in the detection of neurological diseases such as Parkinson's [16]. Similarly, a joint-based approach has shown to be useful in areas such as medical gait analysis [23], [24]. Moreover, an unsupervised learning approach may be inconvenient to the gait identification problem as identities are not labelled during the clustering process. Alternatively, supervised machine learning can conveniently label the identified classes.

A variety of supervised machine learning models have been deployed for gait identification that include Artificial Neural Networks (ANN), Support Vector Machines (SVM), Long Short-Term Memory (LSTM), and KNN as described in Section III. For example, in [17] an LSTM model is used to classify accelerometer data to identify participants, the results are compared to a traditional approach which uses hand-crafted features and a random forest model. The results suggest that the LSTM model outperforms that of the alternative random forest approach when using the hand-crafted

features [17]. A further example of using supervised learning is provided in [18] where a Convolutional Neural Network (CNN) is used to extract features from an IMU sensor network which are then classified using an SVM to identify the participant. Accuracies of 93.36% and 97.06% were achieved, however, this was evaluated using a dataset containing only 10 people [18]. Furthermore, unlike the proposed work, this work uses 5 sensors to provide a whole-body understanding of the motion of the body, such information is not always available in real-world situations as explained in Section I.

Alternatively, [22] presents the R^2-like Similarity (RRS) metric to find the nearest neighbour amongst representative gait templates to achieve person identification. In this work, a smartphone based IMU was used to obtain gait data. Despite demonstrating some success and achieving accuracies up to 89.7%, a significant portion of the errors were associated with a small number of participants [22], suggesting that further research is required to determine whether there is a subset of the population that this approach is unable to identify.

Furthermore, IMUs are increasingly being used to address gait analysis and gait identification problems due to their affordability and ease-of-use [25]. Many of the previously described works make use of wearable sensors, for example, IMUs are used in several works, including in [26], where an IMU is attached to the waist belt of participants to gather gait information. Similarly, in [27] IMUs are attached to the limbs of participants, however, a moving camera is also required to obtain sufficient gait information to recover the body pose of the participants.

Despite the variety of existing works utilising wearable sensors such as IMUs, there is little experimentation with the placement of the sensors. Many works such as [17] and [26] attach the sensor to the trunk of the body or use a network of wearable sensors attached to various parts of the body, as in [18]. This suggests a generic whole-body approach to gait identification which seem appropriate for many applications, particularly when using wearable sensors. However, in some applications, such as when using computer vision, information regarding the whole body is not always available, specifically, occlusion is a major unsolved problem in computer vision-based gait identification [5]. Current sensor-based datasets are not recorded in a way that allows problems such as occlusion to be simulated (*i.e.,* they do not supply independent information regarding individual body parts), thus limiting the use of sensors as a method of prototyping gait identification solutions that could be used to address such problems in the future. To resolve this, the dataset proposed in this work provides data for multiple body joints which provides the potential to simulate real-world problems such as occlusion (*i.e.,* some joints can be withheld to simulate an occluded joint or limb).

Moreover, when there is partial occlusion, other parts of the body are likely to remain visible, therefore, using the limbs or joints that are available at a given time to perform gait identification may offer the opportunity to perform the identification task in the event of partial occlusion. To the best of the authors' knowledge, none of the existing works investigate movement data from individual joints for the purpose of gait identification.

The existing literature also provides examples of alternative sensors for the purpose of gait analysis and identification. For example, in [28] and [29] pressure sensors are attached to foot in order to analyse the wearers' gait pattern. Similarly, in [30] pressure sensors are placed on the floor to identify people walking across it. Alternatively, in [31] and [32] information regarding footsteps is acquired from sounds, the work presented suggests that such an approach may be applicable to the problem of person identification. Despite such solutions demonstrating some degree of success, they are not practical outside of a controlled environment, nor are they able to provide information regarding specific body parts, unlike wearable IMU sensors. Furthermore, due to these limitations, these sensors are not appropriate for prototyping solutions where the aim is to adapt them to computer vision problems, as they do not provide information which can currently be retrieved using existing computer vision methods.

III. METHODOLOGY

The proposed gait identification solution is a composite of several tasks mainly related to the data science cycle as shown in the Figure 1. In the first step, the IMU signal for the body-joints is acquired from real walking sequences of 30 participants. Then the raw data is pre-processed (e.g., cleaned, standardised etc.) using an overlapping (50%) fixed-width window (equivalent to the duration of the average gait cycle). A unique feature vector is then extracted through the overlapped windowing of the data resulting in a large number of statistical features (442 in total). A similar approach is taken in [17], [33], and [34] where it is expected that windowing data in this manner will allow LSTM to learn temporal dependencies between windows which provide complete information regarding a full gait cycle at a given time.

The pre-processed data is then partitioned into two subsets; the training subset contains 80% of the data per participant and is used to train the various machine learning models required. The remaining 20% is reserved and not exposed to the machine learning models until the testing phase. As this is a person identification problem, it is necessary to provide both training and testing data for each participant as such models are unable to identify specific individuals if they have not previously been trained using data associated with that individual.

From the 442 features available, the 30 most important features are identified using feature selection methods including Principal Component Analysis (PCA), the Boruta algorithm, and Recursive Feature Elimination (RFE). In the next step, an LSTM model is trained to identify the relevant participant using the extracted features. Finally, the model is evaluated with varying experimental configurations using the reserved and previously unseen test data (20% of the original data per

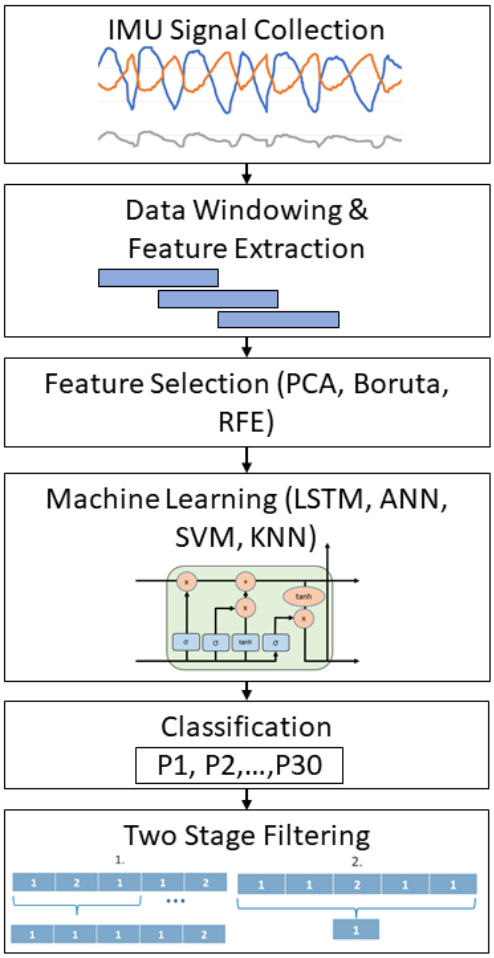

FIGURE 1. Overview of the sequential process of the gait identification methodology presented in this work.

participant is reserved for testing only), here the model is tasked with predicting the participant associated with walking sequences which it has not previously been exposed to. At this stage various alternative machine learning models are also evaluated to provide a comparison to the proposed LSTM model approach. Detailed descriptions of each component in the proposed approach are presented in the following subsections.

A. DATASET COLLECTION

Following the receival of ethical approval from the University Research Ethics Committee (UREC) (Ref: 21/CMP/004), an IMU-based gait dataset has been collected from 30 diverse participants using two synchronised MOTI digital goniometers [35], one attached to the arm and one attached to the leg. Participant recruitment aimed to recruit a diverse range of participants in terms of gender, age, height, weight, and ethnicity, as shown in Table 2. These devices collect movement data related to specific joints depending on the location of the device. The MOTI sensor contains an IMU consisting of an accelerometer, gyroscope, and magnetometer.

TABLE 2. Participant diversity.

	Min	Max	Average
Age	20	65	35.83
Height (cm)	152	188	107.28
Weight (kg)	57	133	79.3

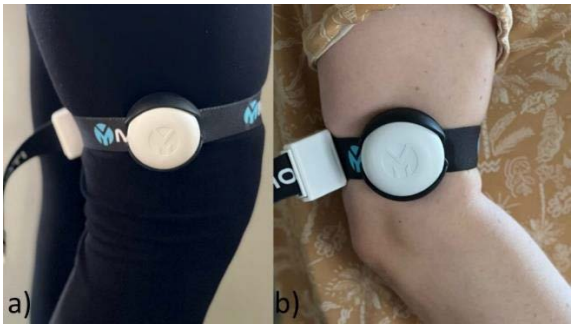

FIGURE 2. MOTI sensor placement, a) leg placement measures hip movement, b) arm placement measures shoulder motion.

Accelerometers measure acceleration the acceleration of the device, gyroscopes measure angular velocity of the device, and magnetometers measure the magnetic field of the Earth [10]. In this work, the device was attached in two positions, as shown in Figure 2. In the first scenario (Figure 2a), the sensor is attached to the right leg above the knee to gain movement data regarding the hip joint while in Figure 2b, the sensor is attached to the right arm above the elbow to obtain movement data regarding the shoulder joint. An adjustable strap is used to comfortably and firmly attach the sensor to the participant, requiring less than 10 seconds to secure the sensor to the participant using the provided clip which can be instantly detached using a button on the clip if required. These joints were chosen for their prominence in the gait cycle, and to provide joints from more than one limb.

Participants were required to perform 12 walking sequences; each was 8 metres in distance and took the participants approximately 6 to 8 seconds on average to complete depending on their walking speed. This provided a total of 240 walking sequences in total, providing approximately 1,680 complete gait cycles, and 120,000 labelled samples. The raw data along with the extracted features is available in the supplementary materials (S1).

B. FEATURE EXTRACTION

Once the dataset is acquired, the next stage is to extract distinct features from the raw data which can be used for the efficient identification of individuals. Firstly, windowing is performed on the recorded data. An average complete gait cycle is empirically selected as an optimal fixed-width window size as shown in Table 3. The average gait cycle is determined by sampling 10 gait cycles from each of the participants in the dataset, the result of which is 0.965 seconds, Table 3 suggests that the optimal window size is equal to the

TABLE 3. A summary of results of the proposed gait identification model with varying window and sample sizes.

Sample Size	Window Size = 0.965(s)	Window Size = 0.4825(s)
1	74.21%	77.17%
5	81.23%	97.66%
10	62.1%	85.36%

TABLE 4. An overview of the data points provided by the MOTI sensor.

Features	Explanation	Units	Range
accX, accY, accZ	Accelerometer data for the X, Y, and Z axis	m/s^2	+/- 9.8
gyrX, gyrY, gyrZ	Gyroscope data for the X, Y, and Z axis	°/s	+/-450
magX, magY, magZ	Magnetometer data for the X, Y, and Z axis	µT	+/- 2,400
Roll, Pitch, Yaw	Euler angles describing 3D orientation	°	0-360
q0, q1, q2, q3	Quaternions describing 3D rotation	Quaternion	+/- 1
MotionDeg	Joint rotation provided in degrees	°	0-360

average full gait cycle (approximately 0.965s in this dataset) which comprises sufficient information in relation to unique patterns of movement. Furthermore, Table 3 also suggests that a sample size of 5 is optimal.

For each overlapping window segment, a feature vector is generated by combining each of the 17 data points provided by the sensor, as described in Table 4, with 13 statistical features, as described in Table 5. As a result, a vector containing 221 features is generated (for leg movement) using overlapped window segmentation. Likewise, we extracted 221 features for the arm movement resulting in 442 features in total.

Table 5 describes the statistical features calculated in each window for each of the data points described in Table 4, as inspired by [33] where similar features are used for an accelerometer only in the detection of the Parkinson's disease symptom, Freezing of fait (FoG). Further detail regarding the range of statistics used can be found in [36]. The features selected in Table 5 provide a range of temporal and spatial features when combined with the data points in Table 4. For example, the maximum, minimum, and mean motion degree provides information regarding the stride length, and kurtosis and skewness provide information regarding the spread of the data. Furthermore, Table 5 includes common time domain features including mean and standard deviation, as well as frequency domain features such as entropy [36].

C. FEATURE SELECTION AND DIMENSIONALITY REDUCTION

Starting with the 442 features as described in Subsection B, a two-stage feature selection stage is performed. Firstly, highly correlated features are removed using PCA to return the features with the highest variance. Secondly, the Boruta

TABLE 5. An overview of the statistical features calculated for each data point in each window.

Features	Description / Formula
Mean	$\frac{\Sigma X}{N}$
Standard Deviation (STD)	$\sqrt{\frac{\Sigma(x_i-\mu)^2}{N}}$
Mean Absolute Deviation (MAD)	$\frac{1}{n}\sum_{i=1}^{n}\lvert x_i - m(X)\rvert$
Maximum	$\max(x_j) - x_{j,n}$
Minimum	$\min(x_j) - x_{j,1}$
Variance (Var)	$\frac{\Sigma(x_i-\bar{x})^2}{n-1}$
Quantile	$F_X(x) := \Pr(X \le x) = p$
Entropy	$\left(1+(X_{1,i}+X_{2,i}+X_{3,i})\right)^2 \times log\left(1+(X_{1,i}+X_{2,i}+X_{3,i})\right)^2$
Max Index	Index of the maximum
Skewness	$\frac{1}{n}\sum_{i=1}^{n}\frac{(x_{j,i}-\bar{x})^3}{S_j^3}$
Kurtosis	$\frac{1}{n}\sum_{i=1}^{n}\frac{(x_{j,i}-\bar{x})^4}{S_j^4}$
Median	$med(x_j) = \begin{cases} x_{j,\frac{n}{2}}, if\ n\ is\ even \\ \frac{x_{j,\frac{n-1}{2}} + x_{j,\frac{n-1}{2}}}{2}, if\ n\ is\ odd \end{cases}$
Standard Error of Mean (SEM)	$\frac{STD}{\sqrt{n}}$

algorithm and RFE are performed on the reduced feature vector. Features selected by both Boruta and RFE are returned to produce the final feature vector containing the most important features. 30 features comprised 80% of the total variance amongst the available feature set, therefore these 30 features were selected as the most important, the same number of features was found to be appropriate in [33].

1) PRINCIPAL COMPONENT ANALYSIS

Principal Component Analysis (PCA) has widely been used as a transformation method [37] as well as method of feature selection, for example, in [38] and [39]. PCA can be used to select the features with the highest importance to the classification task by selecting for high variance, thus ensuring variety in the feature vector [40]. The correlation coefficients between the statistical features extracted from gait data and the principal components (obtained through PCA) is represented by the component loadings in PCA. The maximized sum of variances of the squared loadings is then provided by the component rotations where the absolute sum of component rotations produces importance values (as in Figures 3 and 4 in Appendix) for the corresponding features. In the case of the proposed feature vector, the first 30 PCs cover most of the variance (*i.e.*, almost 80%) and therefore used to calculate the feature importance. The mathematical

TABLE 6. 30 most important features identified during feature selection.

Leg Features	Arm Features
MAD-MotionDeg	Min-Pitch
Max-Pitch	Max-gyrZ
Min-Pitch	Mean-accZ
STD-Yaw	Max-accX
MAD-accX	Max-Pitch
Max-accX	MAD-accY
Mean-accZ	Max-MotionDeg
Median-accZ	Max-accY
MAD-gyrX	Max-gyrX
Max-gyrX	Max-Pitch
Quantile-accZ	MAD-accZ
Var-gyrX	Min-AccZ
Max-gyrY	Median-accZ
Min-gyrX	Min-gyrX
Skewness-gyrY	MAD-gyrZ

formulation of attribute loadings and feature ranking in PCA can be found in [41]

2) BORUTA ALGORITHM

As used in [33], the Boruta algorithm is used for feature selection by identifying the features which are most important for the classification task. The algorithm achieves this by implementing a random forest classifier and iteratively removes features which are deemed statistically less important [42]. The less important features are identified as those which are statistically less relevant than random probes [42]. A detailed explanation of the Boruta algorithm can be found in [42].

3) RECURSIVE FEATURE ELIMINATION (RFE)

As introduced in [43] RFE recursively removes less important features until only the desired number of the most important features remain. At each stage, a machine learning model such as an SVM is trained, each feature is ranked by importance to the output, and finally the least important features are removed [43].

Table 6 presents the 30 most important features (15 for the leg, and 15 for the arm) as identified using the overlapped feature selection methods. Each feature is in the form ''statistical feature–data point'', the corresponding sensor data points and statistical features can be found in Table 4 and Table 5 respectively.

As shown in Table 6, the most commonly appearing sensor data points in the list of most important features are accZ, gyrX, and pitch, suggesting that a range of IMU-based sensors (*i.e.,* containing at least an accelerometer and gyroscope) may be of benefit to similar solutions. Conversely, none of the magnetometer features were selected in the list of the most important features, suggesting that such sensors may be less useful to the gait identification task as compared to the remaining sensors. Furthermore, the most commonly appearing statistical features in the list of most important features are Max, Min, and MAD.

D. CLASSIFICATION

As introduced in [44], LSTM is a type of Recurrent Neural Network (RNN) designed to provide improved results for problems which involve long sequences of data [45]. The main difference between LSTM and RNN is the construction of the LSTM which contains three components. An LSTM cell contains a forget gate which controls how much information is retained, an input gate which updates the values contained in the hidden states, and an output gate which updates the cells output value [45]. For the given task of person identification, the LSTM model is an appropriate model because of the time-series nature of the data involved and the ability of LSTM to learn temporal dependencies between data samples [46].

TABLE 7. LSTM model configuration.

Layer Type	Output Shape	No. Of Parameters
LSTM	100	115200
Dropout	100	0
Dense	100	10100
Dense	30	3030

Table 7 presents the LSTM model configuration implemented in this work; the configuration was selected empirically by repeating the experiment with additional layers until the optimum configuration was found. The optimum configuration contains four layers including an LSTM layer, a dropout layer with a dropout rate of 50% to help prevent overtraining, and two dense layers. The final layer has an output shape of 30 to allow for classification of the 30 participants included in this work. The final output is provided as a single output feature with the range of 1 to 30.

E. ALTERNATIVE APPROACHES

To provide a comparison to the LSTM model which has been implemented in the proposed solution, a variety of popular machine learning models have also been implemented for the classification task. These include an ANN, KNN, and SVM. The following subsections will describe these models and their implementation.

1) ARTIFICIAL NEURAL NETWORK (ANN)

ANNs superficially resemble the neural networks of the human brain. In this work a feed forward ANN has been implemented. In feed forward ANNs, the connections move in one direction only (*i.e.*, forward), unlike RNNs there are no loops in the model which means that inputs are considered in isolation and not in combination with any prior or subsequent inputs [47]. Each node in an ANN computes a function based on its inputs, the result of this function is then passed on to the next nodes in the model [47]. In this work a feed forward ANN has been implemented to classify each of the windowed samples.

2) K-NEAREST NEIGHBOURS

KNNs are a type of instance learning algorithm which performs classifications based on the closest training examples in the feature space [48]. KNNs retain the entire training set, so classification simply involves assigning the majority label of a data points neighbours [48]. In this work, as in [29], the

10 nearest neighbours of the data point to be classified are examined when performing classification. The KNN algorithm is provided in [48].

3) SUPPORT VECTOR MACHINE

The SVMs perform classification tasks by providing an optimal "hyperplane" which separates the members of one class from another [49]. The hyperplane may then be used to predict the most likely classification label for previously unseen data points [49]. Russell and Norvig [47] explain that SVMs provide three main advantages over other supervised learning models. Firstly, they generalize well as a decision boundary with the largest possible distances between points is formed [47]. Secondly, data which cannot be separated linearly can be separated using the kernel trick which uses higher-dimensional space to separate the data [47]. Finally, SVMs have the flexibility to model complex functions whilst being resistant to overfitting, this is due to the fact that SVMs are non-parametric and retain only the knowledge of the points closest to the separating hyperplane [47].

This work used an SVM with a cost=1, a decision function shape of one-vs-one (OVO), and a linear kernel. When using the OVO strategy, the multi-class classification task is broken up into a series of binary classification problems [50]. For this work OVO was chosen over the alternative strategy one-vs-all (OVA), which compares each class against all remaining classes, as it provides improved performance and is less likely to produce imbalanced data [50].

F. FILTERING OF CLASSIFICATION RESULTS

Due to the time-series nature of the dataset, filtering can be used to improve the overall accuracy of the results as predictions can be made using a series of samples produced per participant. For example, given a series of data samples provided by one person, each sample can be classified with respect to the target class (*i.e.,* an individual). Where the predicted classes erroneously belong to more than one class (*i.e.,* multiple persons are predicted where only one is present), filtering can be applied to correct the noisy predictions or make predictions based on relatively larger number of samples (*i.e.*, many consecutive samples from a single walking sequence).

In this work we propose a simple two-stage filtering approach applied after a sequence of data samples have been classified, the algorithm for which is presented in Algorithm 1. Firstly, a moving average is applied whereby every triplet of samples is evaluated, and where there is a mode in the predicted classes (*i.e.,* 2 out of 3, or 3 out of 3 match), the minority class is overwritten with that of the majority. This approach is likely to be affective where accuracy is already high (*i.e.,* $>80\%$) as the chance of predicting the same incorrect class 2 out of 3 times is relatively unlikely. In the case of there being three different classes, the process moves to the next triplet without making changes. Secondly, as this work provides relatively large sequences of data, a final optional step may be taken where the mode is taken across all samples in a sequence (*i.e.,* an entire 8 metre recording sequence for one individual), therefore making a single classification prediction for the entire sequence as opposed to making predictions per sample. This is performed by replacing all sample predictions for that sequence with that of the mode. Both stages of the filtering algorithm are evaluated using the aforementioned reserved test data.

IV. EXPERIMENTAL METHODOLOGY

This work contains three main experiments, the first uses the sensor data for the leg only, the second uses the data for the arm only, and the third uses synchronized data for both the leg and arm. In addition, a further three experiments are provided using the most important selected features, rather

Algorithm 1 Two-Stage Filtering

- Let C be the classifier such that $C \in$ {ANN, LSTM, SVM} used for the prediction for the current frame of feature vector (f)
- Let O be the list of output from C corresponding to each sample S in f
- Sequence (*Seq*) is the complete walking data of one experiment for one person
- Let m be the mode of a sublist
- Let L be the lower limit of the modal class
- Let h be the size of the modal class
- Let f_m be the frequency of the modal class
- Let f_1 be the frequency of the class preceding the modal class
- Let f_2 be the frequency of the class succeeding the modal class

Inputs: Feature Array (f) from Table 5
Output: Predicted Person Identity (p)
Procedure:
For each windowed *Seq* per person:
  For each sample (s) from f:
  - Select the optimal C *(LSTM)*
  - Predicted class (p) =predict(s) using C
  - Store the outcomes p from C in list O

  End Loop
  $$m = L + h\frac{(f_m - f_1)}{(f_m - f_1) + (f_m - f_2)}$$
  If isnull(m):
    Skip
  Else:
    $p = m$
    overwrite p in o
  End If
End Loop

than the large feature vector acquired prior to feature selection. To achieve this, three datasets are created using the aforementioned data, each containing a training set consisting of 80% of the total records for that experiment and a test set containing the remaining 20%. The test set is extracted carefully to ensure that consecutive sequences are extracted (*i.e.,* not random) and remain unseen by the model during the training process.

The aim of these experiments is to test which body joints provide sufficient information to uniquely classify individuals and whether the combination of joints provides improved identification accuracy. Moreover, the additional experiment will demonstrate whether the subset of features deemed the most important are able to provide the same level of identification accuracy as compared to the larger original feature vector. Section III describes the feature extraction approach, which is consistent for all three experiments, note that for the third experiment consisting of the combined data, the feature vector is double that of the feature vector provided by the individual joints (30, as compared to the 15 for the individual joints).

A. EXPERIMENT 1-A (EXP.1-A) LEG ONLY

In Exp.1-A, the motion data from only one of the two MOTI sensors is used (*i.e.,* the one attached to the leg). By calculating each of the 13 statistical features in Table 5 for each of the 17 data points provided in Table 4, 221 potential features are generated for the hip motion. Such an experiment may be used to simulate gait identification under partial occlusion, for example, if the upper body was occluded (*i.e*., by omitting the arm data we may simulate occlusion of the arm).

B. EXPERIMENT 1-B (EXP.1-B) LEG ONLY – SELECTED FEATURES

As in Exp.1-B, only the leg data is used. However, instead of using the entire 221 feature vector, only the most important 15 features are used, as described in Section III.

C. EXPERIMENT 2-A (EXP.2-A) ARM ONLY

In Exp.2-A, the motion data from only one of the two MOTI sensors is used (*i.e.,* the one attached to the arm). By calculating each of the 13 statistical features in Table 5 for each of the 17 data points provided in Table 4, 221 potential features are generated for the shoulder motion. Such an experiment may be used to simulate gait identification under occlusion, for example, if the lower body was occluded (*i.e.,* by omitting the leg sensor data).

D. EXPERIMENT 2-B (EXP.2-B) ARM ONLY – SELECTED FEATURES

As in Exp.2-B, only the arm data is used. However, instead of using the entire 221 feature vector, only the most important 15 features are used, as described in Section III.

E. EXPERIMENT 3-A (EXP.3-A) LEG AND ARM

In Exp.3-A, the motion data from both sensors is used generating 442 potential features (221 for the leg and 221 for the arm). This experiment allows the evaluation of combined joint movements (*i.e.,* simulate no/less occlusion).

F. EXPERIMENT 3-B (EXP.3-B) LEG AND ARM – SELECTED FEATURES

As in Exp.3-A, the data for both the arm and leg is used. However, instead of using the entire 442 feature vector, only the most important 30 features are used, as described in Section III.

V. RESULTS

Following the experimental design (Section IV), statistical results are retrieved from multiple experiments and evaluated using the reserved, previously unseen test data as described in Section III. For each experiment, results of the proposed LSTM model are provided in addition to the alternative models described in Section III, to provide a comparison. Furthermore, the results of both stages of the two-stage filtering algorithm (*i.e.,* the moving average and mode columns), as detailed in Algorithm 1, are presented. Both stages of the filtering algorithm are evaluated using the reserved test data. The first stage of the filtering algorithm, the moving average, is evaluated on a per-sample basis (*i.e.,* many samples per walking sequence). Whereas, due to the nature of the second stage, the mode metric, this is evaluated on a per-sequence basis (*i.e.,* one prediction per walking sequence).

Table 8 presents the results of Exp.1-A, which was completed using leg data only, utilizing all 221 available features. From Table 8 the highest accuracy was achieved using the proposed LSTM approach with an accuracy of 97.3% when evaluated using purely unseen test data. However, the additional metrics, precision, recall, F1 score, and Cohen's Kappa are all highest for the SVM model, suggesting that this may provide a more stable and balanced classification in terms of a reduced rate of false positives.

Table 9 presents the results of Exp.1-B, which was also completed using the leg data only, however, only the 15 most important features were used in this experiment. As in the results from Exp.1-A, the proposed LSTM approach provides the best accuracy. Furthermore, when using only the top 15 as in Exp.1-B, all models report slightly increased results compared to using all features as in Exp.1-A (see Tables 8 and 9), suggesting that an appropriate subset of the original feature vector have been correctly selected.

Table 10 presents the results of Exp.2-A which was completed using the arm data only, using all 221 available features. As with Exp.1-A, the proposed LSTM architecture provides the highest accuracy with 98.9%, the highest reported across all experiments, was achieved when evaluated by using the previously unseen test data. As with experiment 1, the SVM model provided higher scores for the remaining metrics.

Tables 9, 11, and 13 provide the results for Exp.1-B, Exp.2-B, and Exp.3-B respectively, specifically, they provide the results when performed using the most important features only, as described in Section III. The accuracies reported by the LSTM models for the three experiments when using the full feature set and a reduced feature set are very similar, with no more than 1.2% difference. This suggests that the features identified as important in Section III are sufficient for the gait identification task. The novel feature vector presented in Section III may be useful to future IMU-based gait identification works.

Table 11 presents the results of experiment Exp.2-B, which was also completed using the arm data only, using only the 15 most important features. As in the results from Exp.2-A, described in Table 10, LSTM provides the best accuracy, as shown in Table 11. Furthermore, when using only the top features for experiment 2 slightly lower accuracies were reported for all models. However, the difference reported by the LSTM model was only 0.5%.

Table 12 presents the results of Exp.3-A, which was completed using synchronised leg and arm movement data, using all 442 available features. Again, the proposed LSTM architecture provides the highest accuracy with 97.5% achieved when evaluating with previously unseen test data. As with Exp.1-A and Exp.2-A, SVM provided increased results for the additional metrics.

Table 13 presents the results of Exp.3-B, which was also completed using synchronized leg and arm data, using only the 30 most important features. As in the results of Exp.3-A shown in Table 13, LSTM provides the highest accuracy, as shown in Table 13. Furthermore, when using the top features only, the LSTM model accuracy improves by 1.2%, however, all alternative models report lower accuracies as compared to when using the full feature set.

Similar to our proposed solution, an LSTM model is used in [17] to identify the user of a smartphone using accelerometers only. Accuracies of above 90% were achieved using various combinations of the 21 total participants, however, certain combinations of participants provided much lower rates of identification, this is an unexplained issue that the authors expect to be exacerbated with the addition of further participants [17].

In summary of the existing works' results, the accuracies presented in Table 14 shows that the proposed method outperforms the existing similar solutions. Similarly, the LSTM-based solution was shown to outperform the ANN, KNN, and SVM-based alternatives provided as a benchmark comparison for the newly proposed dataset.

Moreover, the results of Exp.1-A, Exp.2-A, and Exp.3-A as presented in Tables 8, 10, and 12 respectively suggest that there is an opportunity to explore joint-based gait identification with a variety of body joints. In each of the experiments the LSTM-based solutions provide the highest accuracies, suggesting that LSTM is an appropriate approach for gait identification using time-series data from individual or combinations of body joints. Exp.2-A, using the arm data only provided the highest accuracy, this is likely due to the more varied arm movement displayed by people, as discussed in Section IV. This suggests that there is an opportunity to further explore arm movement and joint movement to contrast the traditional approaches which focus on either the legs or the trunk of the body.

VI. DISCUSSIONS

As shown in Section V, each trained model (when evaluated over unseen instances) indicated a higher accuracy for the arm data (Exp.2-A) as compared to the leg data (Exp.1-A). This is likely due to the more obvious differentiations in arm movements that can be visually observed. For example, some people are rigid and have very little arm movement when they walk, some people allow their arms to naturally swing with the rhythm of their walking, and some people use more energy and swing their arms more flamboyantly as they walk [11].

Furthermore, it can be observed that overall, the results of Exp.2-A, arm data only, provided higher accuracy than those of Exp.3-A, the combination of leg and arm data. This was an unexpected result as it was anticipated that the unique traits of both limbs would provide more unique gait traits for each participant.

As presented in Section V, Table 14 compares the accuracy of proposed solution to those of similar IMU-based gait identification works from the literature. In [19], movement data was gathered from 24 participants via an IMU device attached to the ankle, containing an accelerometer and gyroscope, but unlike in the proposed work, it does not include a magnetometer which would provide additional features. A CNN is used in [19] to perform feature extraction, from which an SVM classifies participants. An accuracy of 80% is reported when provided with data containing 5 complete gait cycles. In contrast, we use window size equivalent to a single complete gait cycle and a sample size of 5 windows achieving an accuracy of up to 98.9% using a similar amount of data, as shown in Table 10. Furthermore, the use of a CNN for feature extraction in [19], as compared to our hand-crafted features, will limit the explain-ability and interpretability of the model [51].

Similarly, in [20] IMU data was gathered from 30 participants via a smartphone attached to the trunk of the body. As in [19], magnetometer and gyroscope data was not included, both of which may provide useful features, as demonstrated in our proposed solution. As described in section II, attaching the sensor to the trunk means that only generic whole-body data is provided, and does not allow for the evaluation of individual limbs and joints, unlike the proposed work. Furthermore, the approach described in [20] used the same number of participants as in the proposed solution but achieved only 80.3% accuracy, considerably lower than that the 98.9% we report in Table 14.

Unlike the other works described in Table 14 and our proposed solution, [18] gathers movement data using a network of 5 IMU sensors. Despite only containing 10 participants,

TABLE 8. Results of experiment 1A, using leg data only (Exp.1-A).

Model	Accuracy	Precision	Recall	F1 Score	Kappa	Moving Average	Mode
ANN	86%	59.7%	59%	58.5%	55.4%	86.67%	100%
KNN	72.9%	75.3%	73.8%	72.1%	71.9%	74.21%	83.33%
SVM	94.4%	94.9%	94.3%	94.4%	94.3%	94.46%	100%
LSTM	97.3%	85.7%	69.4%	70.4%	71.3%	97.34%	100%

TABLE 9. Results of experiment 1B, using leg data only (top 15 features only) (Exp.1-B).

Model	Accuracy	Precision	Recall	F1 Score	Kappa	Moving Average	Mode
ANN	85.36%	54.31%	52.72%	52.44%	51.8%	87.3%	93.3%%
KNN	66.89%	70.46%	66.28%	66.44%	65.61%	67.5%	83.33%
SVM	74.44%	76.55%	74.36%	74.15%	73.5%	75.27%	100%
LSTM	98.23%	86.94%	71.46%	71.31%	71.91	98.64%	100%

TABLE 10. Results of Experiment 2A, using arm data only (Exp.2-A).

Model	Accuracy	Precision	Recall	F1	Kappa	Moving Average	Mode
ANN	86.1%	62.6%	62.3%	61.7%	57.1%	87.13%	100%
KNN	81%	82%	81.8%	80.1%	80.2%	81.37%	93.3%
SVM	95.7%	95%	95%	94.8%	95.5%	95.77%	100%
LSTM	98.9%	93.4%	84.3%	78.8%	81.2%	98.9%	100%

TABLE 11. Results of Experiment 2B, using arm data only (top 15 features only) (exp.2-b).

Model	Accuracy	Precision	Recall	F1	Kappa	Moving Average	Mode
ANN	78.4%	69.24%	69.05%	67.62 %	67.29%	78.76%	93.3%
KNN	77.61%	80.1%	77.97%	77.12%	76.77%	78.3%	93.3%
SVM	79.39%	81.62%	80.75%	80.21%	78.59%	80.16%	100%
LSTM	98.33%	93.33%	83.2%	77.96%	81.78%	98.37%	100%

TABLE 12. Results of experiment 3A, using synchronised leg and arm data (Exp.3-A).

Model	Accuracy	Precision	Recall	F1	Kappa	Moving Average	Mode
ANN	86.1%	61.9%	62.3%	61.9%	57.8%	87.21%	100%
KNN	88.4%	89.9%	88.3%	88.2%	88%	90.02%	100%
SVM	96.2%	98.4%	98.2%	98.3%	98.2%	97.1%	100%
LSTM	97.5%	89%	79.8%	77.6%	80.7%	97.52%	100%

TABLE 13. Results of experiment 3B, using synchronised leg and arm (top 30 features only) (Exp.3-B).

Model	Accuracy	Precision	Recall	F1	Kappa	Moving Average	Mode
ANN	77.8%	79.09%	79.93%	78.47%	76.96%	79.1%	100%
KNN	89.78%	90.36%	89.1%	88.86%	89.41%	89.81%	100%
SVM	92.44%	93.06%	92.7%	92.57%	92.16%	92.65%	100%
LSTM	98.68%	90.38%	82.27%	79.76%	80.72%	98.73%	100%

an accuracy of 91% is reported, which is substantially lower than the 98.9% achieved by the proposed work which contains 30 participants and requires fewer sensors.

In [21] motion data was collected using a smartphone and 3 IMU sensors attached to the waist for a total of 744 participants [21]. Using this dataset [21] reports 97.16% accuracy, slightly lower than that reported in our work. However, similar to [19], this solution relies on a CNN for feature extraction. Again, unlike the statistical features used in the proposed work, CNN-based feature extraction would likely make the model less explainable. Furthermore, only the preprocessed dataset is available, not the original raw data, thus limiting the ability to reuse or experiment the original data. Furthermore, similar to [20], the sensor used in [21] was attached to the trunk. Again, this provides motion data for the body as a whole and does not allow for limb or joint-based approaches

TABLE 14. A comparison of IMU-based gait identification works.

Ref	No. Participants	Sensor Placement	Model	Accuracy
[19]	24	Ankle	CNN / SVM	80%
[20]	30	Trunk	GMM-UBM	80.3%
[18]	10	Network	CNN	91%
[21]	744	Trunk	CNN	97.16%
[17]	21	Trunk	LSTM	90%
Ours (Exp.1-B)	30	Leg	LSTM	97.3%
Ours (Exp.2-B)	30	Arm	LSTM	98.9%
Ours (Exp.3-B)	30	Leg & Arm	LSTM	97.5%

to be implemented or evaluated. A further limitation with the dataset used is the fact that only 2.5 seconds of data is recorded per participant, thus limiting the number of complete gait cycles [52]. In comparison, we provide approximately 60 seconds of data per participant in our primary dataset.

Overall, in all experiments, the proposed LSTM model outperformed the alternatives, achieving classification accuracy of up to 98.9%. In addition, reducing the feature vector by more than 93% did not reduce the performance, and in 2 out of three experiments, the feature vector reduction lead to improved classification accuracy. The results of the two-stage filtering approach described in Algorithm 1, as shown in Tables 8, 9, 10, 11, 12, and 13, suggest that it leads to improved results where longer walking sequences (*e.g.*, 8 metres in this case). The success of the mode metric is in part due to the high accuracies achieved during the initial prediction. As accuracies of up to 98.9% were achieved when evaluating the predicted samples, the mode (per sequence) must be correct as most of the samples within each sequence are correctly predicted, thus leading to the 100% accuracy achieved in some experiments by the mode metric. However, further work and more data is required to further validate the mode metric as each walking sequence provides only a single prediction to validate when using this approach.

The aforementioned statistical performance clearly validates the proposed proof-of-concept that can be a baseline to further explore it for a computer vision-based implementation. This paper demonstrates that when provided with accurate joint angles, a high accuracy of gait-based identification is achievable. Therefore, it is likely that a high accuracy of identification can be expected from future vision-based implementations if the joint-angle can be accurately estimated using computer vision methods. Computer vision provides the potential for more practical implementations, for example, for security and policing it can be performed covertly, without the cooperation of the subjects. Such an implementation may also help to address the problem of occlusion that affects many of the current computer vision-based approaches to gait identification, this is possible as except for in cases of total occlusion, there is likely to be at least one or more body joints visually available for the purpose of gait-based identification. As demonstrated in this work, a single joint may provide enough information to accurately identify an individual.

It is also important to note that the related problem of gait identification when unknown people have been detected (*i.e.,* those not in the training set or those that we do not seek to identify) should be addressed to improve the real-world implication of the proposed solution. For example, when searching for missing people, the solution should exclude people who are not on the missing persons list (*i.e.,* do not attempt to identify them). To the best of the authors' knowledge, this is an important area of research which has gained little attention and therefore a robust solution is not currently available. One potential solution, OpenMax [53], is an alternative final layer for machine learning models which aims to estimate the probability of a sample belonging to an unknown class. It achieves this by adapting SoftMax and removes the requirement for probabilities over all classes to sum to 1 and includes a category for the unknown classes [53]. However, the implementation and evaluation of this would require the collection of gait data from additional participants to act as the unknown classes, as to the best of the authors' knowledge, such an open set gait dataset is not currently available.

Furthermore, the authors are not aware of any existing works exploring how person identification can be performed using pathological gait (*i.e.,* gait abnormalities caused by pain, reduced range-of-motion, or weakness, for example) or where the person has aged significantly since their gait sample was collected. As current works utilize datasets captured over a relatively brief period, the data provides information regarding the person's gait at the time of recording, and therefore does not account for future, ageing, injury, or illness. Matovski *et al.* [54] report that the effect of time between recording session has less impact on identification accuracy than other factors such as clothing. However, the dataset collected contains only a single six-month gap between recordings, and the authors are not aware of any alternative gait datasets with time gaps between recordings. An initial approach to further explore this problem would require the collection of a gait dataset recorded at significant intervals (*i.e.,* years) containing instances of pathological gait. It may then be possible to identify unaffected gait features which may aid in person identification from pathological gait data. Solving this problem would potentially create an identification system capable of identifying individuals long after their gait samples have been collected, without the requirement of updating the gait data for each participant.

VII. CONCLUSION AND FUTURE WORK

This work has demonstrated that both the hip and shoulder joint movements on their own as well as in combination possess sufficient information to provide accurate gait-based

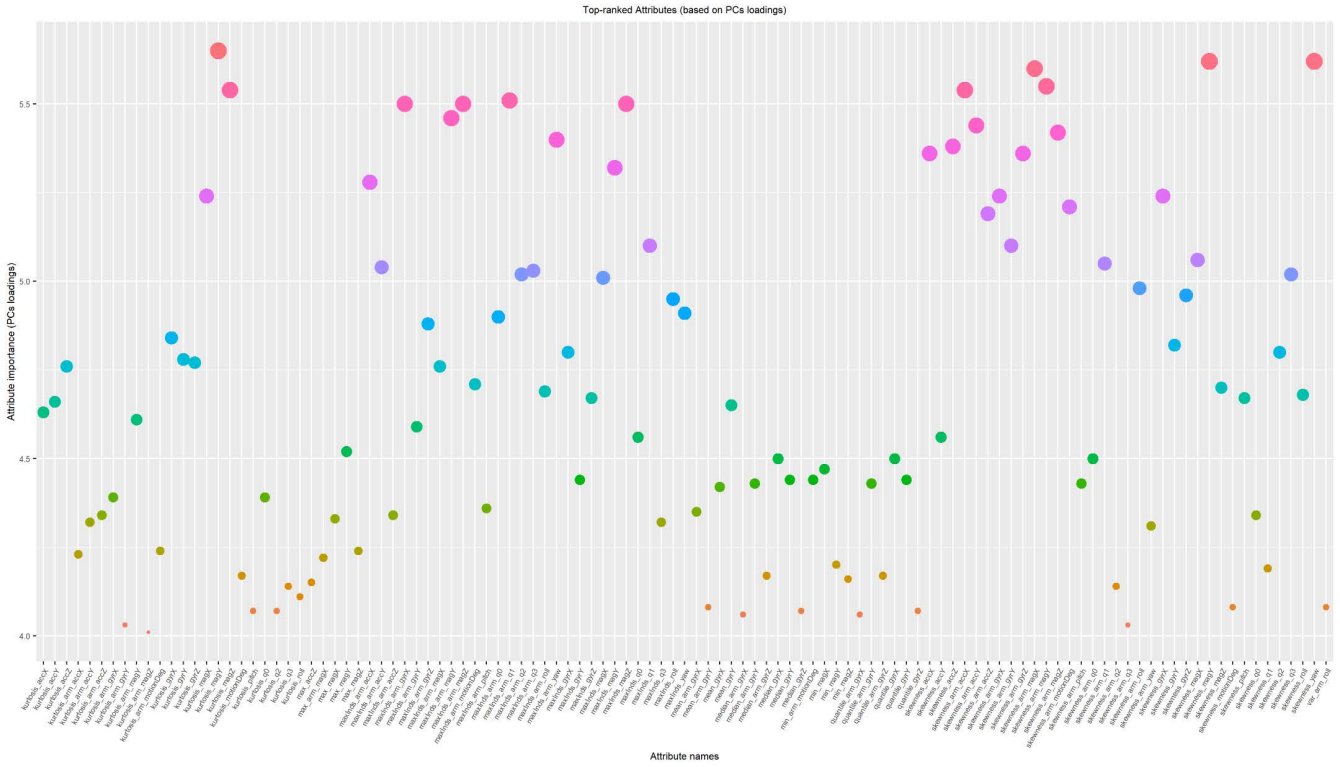

FIGURE 3. Top Quartile (25% most important features) based on their importance.

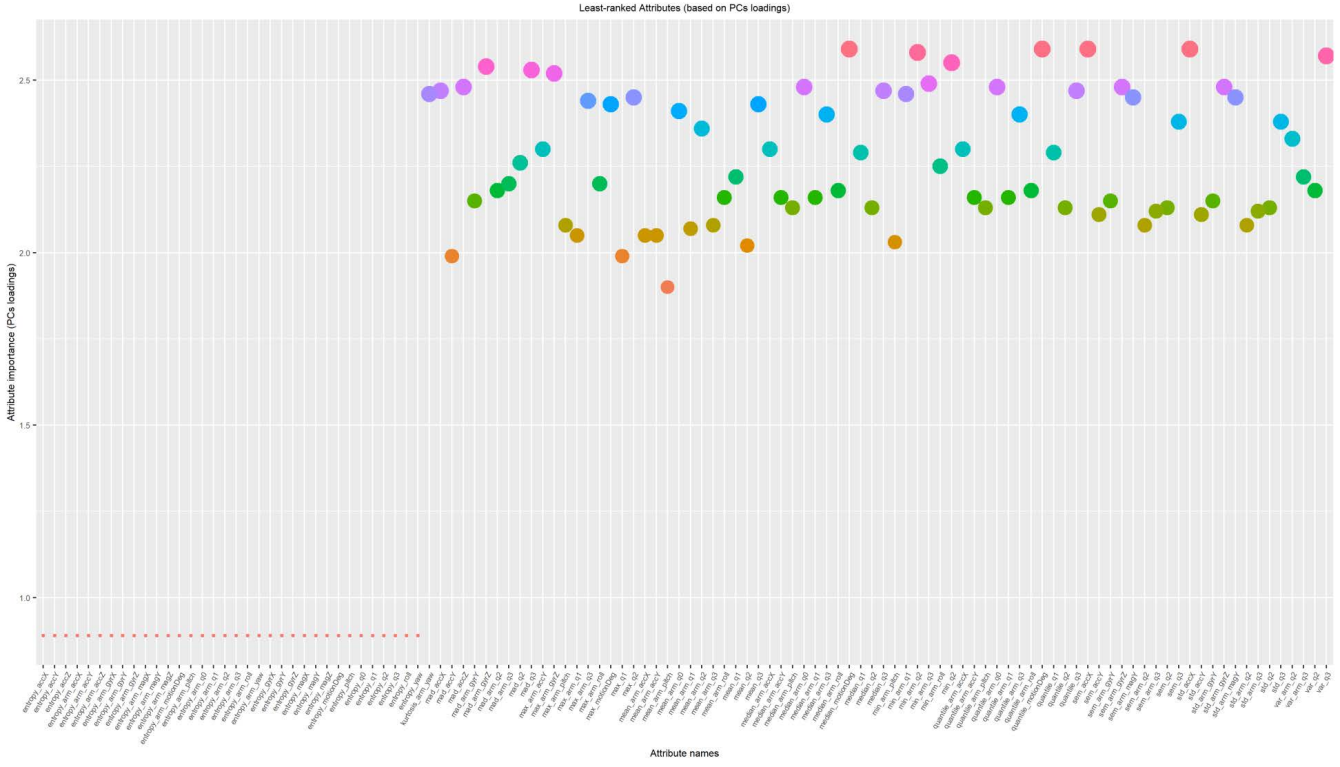

FIGURE 4. 1st Quartile (25% least-important features) based on their importance.

identification. To the best of the authors' knowledge, a single joint has not been used for gait identification in previous works. These findings present the opportunity for future developments in joint-based gait identification which could potentially help to overcome the problem of occlusion in computer vision-based gait identification and therefore, help

reduce false positive identifications. Future work is required to implement this approach in computer vision, and also to develop the necessary algorithms to make predictions based on the subset of available joints in the event of occlusion occurring.

Using the feature selection approach described in Section III, the 30 most important features from the available 442 are presented in Table 6. Moreover, the most important features contain features from two of the IMU sensors (gyroscope and accelerometer). Therefore, including a variety of sensors will likely be beneficial for future works, as this is not always applied in the literature, for example, [19] does not use a gyroscope.

The simple filtering method based on the moving-average and mode as described in Algorithm 1 (Section III) has improved the accuracies in almost all cases as shown in Tables 8, 9, 10, 11, 12, and 13. Often, accuracies of 100% are reported by a variety of models when presented with a full walking sequence (8 metres) per person. Furthermore, it should be noted that 8 metres is a relatively large walking distance to obtain, and it is therefore likely that this amount of data would not be available in many circumstances, for instance, security camera footage in a small shop with limited walking space, therefore, the mode metric may be deemed an optional additional step.

Future work is planned to extend the gait dataset to include additional participants, the aim is to collect data for 100 diverse (in terms of gender, age, height, weight, ethnicity etc.) participants. Such a dataset would increase the generalisation of our proposed models and would increase the confidence in the identification results and filtering approach. When the dataset is complete, we plan to upload it and to share it with the wider research community. The expanded dataset will provide the opportunity to address questions such as whether anthropometric and demographic parameters influence the ability to identify participants using the proposed and alternative solutions. For example, by comparing the success of gait identification models on the proposed diverse dataset to that of less diverse datasets currently available.

Furthermore, in addition to the leg and arm data, we also collected the head movements during the walk. Future work is planned to investigate whether the movement of the head provides relevant information for the task of person identification. This experiment was inspired by the observation that in many busy and heavily crowded areas it is sometimes only possible to see people's heads when their bodies are occluded by people in front of them. Such a solution would provide the opportunity for gait-based identification in crowded and heavily occluded environments such as city centers. Finally, the proposed approach sets the baseline for computer vision-based gait identification which is more practical to overcome the challenges of limited cooperation from the subjects and the problem of occlusion affecting many of the current computer vision-based approaches to gait identification.

APPENDIX (A1)—PCA

See Figures 3 and 4.

ACKNOWLEDGMENT

The authors wish to extend gratitude to all the participants who volunteered to be included in our gait dataset.

REFERENCES

[1] C. Fox. (2018). *Face Recognition Police Tools 'Staggeringly Inaccurate'*. BBC News. Accessed: Mar. 24, 2022. [Online]. Available: https://www.bbc.co.uk/news/technology-44089161

[2] J. Sharman. (2018). *Metropolitan Police'S Facial Recognition Technology 98% Inaccurate, Figures Show*. Independent. Accessed: Mar. 24, 2022. [Online]. Available: https://www.independent.co.uk/news/uk/home-news/met-police-facial-recognition-success-south-wales-trial-home-office-false-positive-a8345036.html

[3] M. Burgess. *Facial Recognition Tech Used by UK Police is Making a Ton of Mistakes*. WIRED. Accessed: Mar. 24, 2022. [Online]. Available: https://www.wired.co.uk/article/face-recognition-police-uk-south-wales-met-notting-hill-carnival

[4] G. Guo and N. Zhang, "A survey on deep learning based face recognition," *Comput. Vis. Image Understand.*, vol. 189, Dec. 2019, Art. no. 102805, doi: 10.1016/j.cviu.2019.102805.

[5] J. P. Singh, S. Jain, S. Arora, and U. P. Singh, "Vision-based gait recognition: A survey," *IEEE Access*, vol. 6, pp. 70497–70527, 2018, doi: 10.1109/ACCESS.2018.2879896.

[6] J. Wen, Y. Shen, and J. Yang, "Multi-view gait recognition based on generative adversarial network," *Neural Process. Lett.*, vol. 54, no. 3, pp. 1855–1877, Jun. 2022, doi: 10.1007/s11063-021-10709-1.

[7] L. K. Topham, W. Khan, D. Al-Jumeily, and A. Hussain, "Human body pose estimation for gait identification: A comprehensive survey of datasets and models," *ACM Comput. Surveys*, early access, May 2022. [Online]. Available: https://dl.acm.org/doi/10.1145/3533384

[8] C. Wan, L. Wang, and V. V. Phoha, "A survey on gait recognition," *ACM Comput. Surv.*, vol. 51, no. 5, pp. 1–35, 2018, doi: 10.1145/3230633.

[9] M. De Marsico and A. Mecca, "A survey on gait recognition via wearable sensors," *ACM Comput. Surv.*, vol. 52, no. 4, pp. 1–39, 2019, doi: 10.1145/3340293.

[10] N. Ahmad, R. A. R. Ghazilla, N. M. Khairi, and V. Kasi, "Reviews on various inertial measurement unit (IMU) sensor applications," *Int. J. Signal Process. Syst.*, vol. 1, no. 2, pp. 256–262, 2013, doi: 10.12720/ijsps.1.2.256-262.

[11] J. E. Cutting and L. T. Kozlowski, "Recognizing friends by their walk: Gait perception without familiarity cues," *Bull. Psychonomic Soc.*, vol. 9, no. 5, pp. 353–356, May 1977, doi: 10.3758/BF03337021.

[12] S. V. Stevenage, M. S. Nixon, and K. Vince, "Visual analysis of gait as a cue to identity," *Appl. Cogn. Psychol.*, vol. 13, pp. 513–526, Dec. 1999, doi: 10.1002/(SICI)1099-0720(199912)13:6<513::AID-ACP616>3.0.CO;2-8.

[13] M. Popovic, T. Keller, and S. Ibrahim, "Gait identification and recognition sensor," in *Proc. 6th Vienna Int. Workshop Funct. Electrostimulation*, Dec. 2012, pp. 1–4.

[14] G. Cola, M. Avvenuti, A. Vecchio, G. Z. Yang, and B. Lo, "An unsupervised approach for gait-based authentication," in *Proc. IEEE 12th Int. Conf. Wearable Implantable Body Sensor Netw. (BSN)*, Jun. 2015, pp. 1–6, doi: 10.1109/BSN.2015.7299423.

[15] M. Yuwono, S. W. Su, Y. Guo, B. D. Moulton, and H. T. Nguyen, "Unsupervised nonparametric method for gait analysis using a waist-worn inertial sensor," *Appl. Soft Comput.*, vol. 14, pp. 72–80, Jan. 2014, doi: 10.1016/j.asoc.2013.07.027.

[16] N. Roth, A. Küderle, M. Ullrich, T. Gladow, F. Marxreiter, J. Klucken, B. M. Eskofier, and F. Kluge, "Hidden Markov model based stride segmentation on unsupervised free-living gait data in Parkinson's disease patients," *J. NeuroEngineering Rehabil.*, vol. 18, no. 1, pp. 1–15, Dec. 2021, doi: 10.1186/s12984-021-00883-7.

[17] Y. Watanabe and M. Kimura, "Gait identification and authentication using LSTM based on 3-axis accelerations of smartphone," *Proc. Comput. Sci.*, vol. 176, pp. 3873–3880, 2020, doi: 10.1016/j.procs.2020.09.001.

[18] O. Dehzangi, M. Taherisadr, and R. ChangalVala, "IMU-based gait recognition using convolutional neural networks and multi-sensor fusion," *Sensors*, vol. 17, no. 12, p. 2735, Nov. 2017, doi: 10.3390/s17122735.

[19] M. Gadaleta, L. Merelli, and M. Rossi, "Human authentication from ankle motion data using convolutional neural networks," in *Proc. IEEE Stat. Signal Process. Workshop (SSP)*, Jun. 2016, pp. 1–5, doi: 10.1109/SSP.2016.7551815.
[20] R. San-Segundo, J. D. Echeverry-Correa, C. Salamea-Palacios, S. L. Lutfi, and J. M. Pardo, "I-vector analysis for gait-based person identification using smartphone inertial signals," *Pervas. Mob. Comput.*, vol. 38, pp. 140–153, May 2017, doi: 10.1016/j.pmcj.2016.09.007.
[21] H. Huang, P. Zhou, Y. Li, and F. Sun, "A lightweight attention-based CNN model for efficient gait recognition with wearable IMU sensors," *Sensors*, vol. 21, no. 8, pp. 1–13, 2021, doi: 10.3390/s21082866.
[22] S. Deb, Y. O. Yang, M. C. H. Chua, and J. Tian, "Gait identification using a new time-warped similarity metric based on smartphone inertial signals," *J. Ambient Intell. Humanized Comput.*, vol. 11, no. 10, pp. 4041–4053, Oct. 2020, doi: 10.1007/s12652-019-01659-7.
[23] M. Abid, N. Mezghani, and A. Mitiche, "Knee joint biomechanical gait data classification for knee pathology assessment: A literature review," *Appl. Bionics Biomechanics*, vol. 2019, pp. 1–14, May 2019, doi: 10.1155/2019/7472039.
[24] L. E. C. Lizama, F. Khan, P. V. Lee, and M. P. Galea, "The use of laboratory gait analysis for understanding gait deterioration in people with multiple sclerosis," *Multiple Sclerosis J.*, vol. 22, no. 14, pp. 1768–1776, Dec. 2016, doi: 10.1177/1352458516658137.
[25] S. F. Castiglia, D. Trabassi, A. Tatarelli, A. Ranavolo, T. Varrecchia, L. Fiori, D. D. Lenola, E. Cioffi, M. Raju, G. Coppola, P. Caliandro, C. Casali, and M. Serrao, "Identification of gait unbalance and fallers among subjects with cerebellar ataxia by a set of trunk acceleration-derived indices of gait," *Cerebellum*, pp. 1–13, Jan. 2022. [Online]. Available: https://link.springer.com/article/10.1007/s12311-021-01361-5, doi: 10.1007/s12311-021-01361-5.
[26] N. Hajati and A. Rezaeizadeh, "A wearable pedestrian localization and gait identification system using Kalman filtered inertial data," *IEEE Trans. Instrum. Meas.*, vol. 70, pp. 1–8, 2021, doi: 10.1109/TIM.2021.3073440.
[27] T. von Marcard, R. Henschel, M. J. Black, B. Rosenhahn, and G. Pons-Moll, "Recovering accurate 3D human pose in the wild using IMUs and a moving camera," in *Proc. Eur. Conf. Comput. Vis.*, vol. 11214, 2018, pp. 614–631, doi: 10.1007/978-3-030-01249-6_37.
[28] W. Si, G. Yang, X. Chen, and J. Jia, "Gait identification using fractal analysis and support vector machine," *Soft Comput.*, vol. 23, no. 19, pp. 9287–9297, Oct. 2019, doi: 10.1007/s00500-018-3609-8.
[29] M. N. Alam, A. Garg, T. T. K. Munia, R. Fazel-Rezai, and K. Tavakolian, "Vertical ground reaction force marker for Parkinson's disease," *PLoS ONE*, vol. 12, no. 5, pp. 1–13, 2017, doi: 10.1371/journal.pone.0175951.
[30] R. V. Rodriguez, N. Evans, and J. S. D. Mason, "Footstep recognition," in *Encyclopedia Biometrics*. Boston, MA, USA: Springer, 2015, pp. 693–700.
[31] F. Liu and Q. Jiang, "Research on recognition of criminal suspects based on foot sounds," in *Proc. IEEE 3rd Inf. Technol., Netw., Electron. Autom. Control Conf. (ITNEC)*, Mar. 2019, pp. 1347–1351, doi: 10.1109/ITNEC.2019.8729307.
[32] E. Aydemir, T. Tuncer, S. Dogan, and M. Unsal, "A novel biometric recognition method based on multi kernelled bijection octal pattern using gait sound," *Appl. Acoust.*, vol. 173, Feb. 2021, Art. no. 107701, doi: 10.1016/j.apacoust.2020.107701.
[33] N. Kleanthous, A. J. Hussain, W. Khan, and P. Liatsis, "A new machine learning based approach to predict freezing of gait," *Pattern Recognit. Lett.*, vol. 140, pp. 119–126, Dec. 2020, doi: 10.1016/j.patrec.2020.09.011.
[34] S. Sony, S. Gamage, A. Sadhu, and J. Samarabandu, "Vibration-based multiclass damage detection and localization using long short-term memory networks," *Structures*, vol. 35, pp. 436–451, Jan. 2022, doi: 10.1016/j.istruc.2021.10.088.
[35] *MOTI*. Accessed: Apr. 12, 2022. [Online]. Available: https://moti.dk
[36] N. Kleanthous, A. J. Hussain, W. Khan, J. Sneddon, A. Al-Shammaa, and P. Liatsis, "A survey of machine learning approaches in animal behaviour," *Neurocomputing*, vol. 491, pp. 442–463, Jun. 2022, doi: 10.1016/j.neucom.2021.10.126.
[37] F. Song, Z. Guo, and D. Mei, "Feature selection using principal component analysis," in *Proc. Int. Conf. Syst. Sci., Eng. Design Manuf. Informatization*, Nov. 2010, pp. 27–30, doi: 10.1109/ICSEM.2010.14.
[38] A. Larumbe, M. Ariz, J. J. Bengoechea, R. Segura, R. Cabeza, and A. Villanueva, "Improved strategies for HPE employing Learning-by-Synthesis approaches," in *Proc. IEEE Int. Conf. Comput. Vis. Workshops (ICCVW)*, Oct. 2017, pp. 1545–1554, doi: 10.1109/ICCVW.2017.182.
[39] W. Khan, K. Crockett, J. O'Shea, A. Hussain, and B. M. Khan, "Deception in the eyes of deceiver: A computer vision and machine learning based automated deception detection," *Exp. Syst. Appl.*, vol. 169, May 2021, Art. no. 114341, doi: 10.1016/j.eswa.2020.114341.
[40] A. K. Gárate-Escamila, A. Hajjam El Hassani, and E. Andrès, "Classification models for heart disease prediction using feature selection and PCA," *Informat. Med. Unlocked*, vol. 19, 2020, Art. no. 100330, doi: 10.1016/j.imu.2020.100330.
[41] H. Abdi and L. J. Williams, "Principal component analysis," *Wiley Interdiscipl. Rev., Comput. Statist.*, vol. 2, no. 4, pp. 433–459, 2010, doi: 10.1002/wics.101.
[42] M. B. Kursa and W. R. Rudnicki, "Feature selection with the Boruta package," *J. Stat. Softw.*, vol. 36, no. 11, pp. 1–13, 2010, doi: 10.18637/jss.v036.i11.
[43] I. Guyon, J. Weston, S. Barnhill, and V. Vapnik, "Gene selection for cancer classification using support vector machines," *Mach. Learn.*, vol. 46, nos. 1–3, pp. 389–422, 2002, doi: 10.1007/978-3-540-88192-6_8.
[44] S. Hochreiter and J. Schmidhuber, "Long short-term memory," *Neural Comput.*, vol. 9, no. 8, pp. 1735–1780, 1997.
[45] C. F. G. dos Santos, D. D. S. Oliveira, L. A. Passos, R. G. Pires, D. F. S. Santos, L. P. Valem, T. P. Moreira, M. Cleison S. Santana, M. Roder, J. P. Papa, and D. Colombo, "Gait recognition based on deep learning: A survey," *ACM Comput. Surveys*, vol. 55, no. 2, pp. 1–34, Mar. 2023, doi: 10.1145/3490235.
[46] Y. Luo, J. Ren, Z. Wang, W. Sun, J. Pan, J. Liu, J. Pang, and L. Lin, "LSTM pose machines," in *Proc. IEEE/CVF Conf. Comput. Vis. Pattern Recognit.*, Jun. 2018, pp. 5207–5215.
[47] S. Russell and P. Norvig, *Artificial Intelligence: A Modern Approach*, Global Ed., 4th ed. London, U.K.: Pearson, 2021.
[48] S. B. Imandoust and M. Bolandraftar, "Application of K-nearest neighbor (KNN) approach for predicting economic events: Theoretical background," *Int. J. Eng. Res. Appl.*, vol. 3, no. 5, pp. 605–610, 2013.
[49] D. A. Pisner and D. M. Schnyer, "Support vector machine," in *Machine Learning: Methods and Applications to Brain Disorders*. Amsterdam, The Netherlands: Elsevier, 2019, pp. 101-121.
[50] M. Galar, A. Fernández, E. Barrenechea, H. Bustince, and F. Herrera, "An overview of ensemble methods for binary classifiers in multi-class problems: Experimental study on one-vs-one and one-vs-all schemes," *Pattern Recognit.*, vol. 44, no. 8, pp. 1761–1776, Aug. 2011, doi: 10.1016/j.patcog.2011.01.017.
[51] A. S. Wicaksana and C. C. S. Liem, "Human-explainable features for job candidate screening prediction," in *Proc. IEEE Conf. Comput. Vis. Pattern Recognit. Workshops (CVPRW)*, Jul. 2017, pp. 1664–1669, doi: 10.1109/CVPRW.2017.212.
[52] H. Iwama, M. Okumura, Y. Makihara, and Y. Yagi, "The OU-ISIR gait database comprising the large population dataset and performance evaluation of gait recognition," *IEEE Trans. Inf. Forensics Security*, vol. 7, no. 5, pp. 1511–1521, Oct. 2012, doi: 10.1186/s41074-017-0035-2.
[53] A. Bendale and T. E. Boult, "Towards open set deep networks," in *Proc. IEEE Conf. Comput. Vis. Pattern Recognit. (CVPR)*, Dec. 2016, pp. 1563–1572, doi: 10.1109/CVPR.2016.173.
[54] D. S. Matovski, M. S. Nixon, S. Mahmoodi, and J. N. Carter, "The effect of time on gait recognition performance," *IEEE Trans. Inf. Forensics Security*, vol. 7, no. 2, pp. 543–552, Apr. 2012, doi: 10.1109/TIFS.2011.2176118.

LUKE K. TOPHAM received the B.Sc. degree in computer science from the University of Chester, in 2014, the M.Sc. degree in computer science from Liverpool John Moores University, in 2015, and the M.Phil. degree in engineering from the University of Liverpool, in 2020. He is currently pursuing the Ph.D. degree in computer science with Liverpool John Moores University.

From 2015 to 2016, he worked as a Research Assistant at Liverpool John Moores University. Between 2016 and 2021, he was a further Education Lecturer. His current research interests include gait identification using computer vision and machine learning.

WASIQ KHAN (Member, IEEE) received the Ph.D. degree in AI and speech processing from Bradford University, U.K., in 2015. He is currently a Senior Lecturer in artificial intelligence and lead academic in data sciences with the Department of Computer Science, Liverpool John Moores University, U.K. He is research active within the domain of AI/machine learning, video/speech data processing, and data science. He has been working as a Lead on various large-scale research projects in collaborations with academia and industry mainly related to applied AI and pattern matching. He has published over 50 peer-reviewed research articles within the high-ranked journals and conferences. He is an active member of several professional bodies, including IEEE and ACM, and a reviewer of various top-ranked journals, including IEEE TRANSACTIONS. Along with his Ph.D. supervisions and academic roles, he has established academic citizenship within the domain of AI and data science. He is also a fellow of HEA and a member of the Computational Intelligence Society.

DHIYA AL-JUMEILY (Senior Member, IEEE) is currently a Professor in artificial intelligence with Liverpool John Moores University and the President of the e-Systems Engineering Society. He has extensive research interests include the wide variety of interdisciplinary perspectives concerning the theory and practice of applied artificial intelligence in medicine, human biology, intelligent community, and health care. He has published over 300 peer-reviewed scientific international publications, ten books, and seven book chapters, in multidisciplinary research areas, including machine learning, neural networks, signal prediction, telecommunication fraud detection, AI-based clinical decision-making, medical knowledge engineering, human–machine interaction, intelligent medical information systems, sensors and robotics, wearable and intelligent devices, and instruments. But his current research passion is decision support systems for self-management of health and medicine. He is also a Chartered IT Professional. He is also a fellow of the U.K. Higher Education Academy. He is also a Senior Member of OBE.

ATIF WARAICH is currently the Director of the School of Computer Science and Mathematics, Liverpool John Moores University (LJMU). Prior to joining LJMU (in June 2017) he was the Head of the Division of Digital Media and Entertainment technology, Manchester Metropolitan University (MMU), and also the Enterprise Lead and was the Founder and the Director of the Manchester Usability Laboratory. His research interests include several areas the first is the use of technology to enhance learning, specifically he is interested in how game like environments can be used to promote learning and to motivate learners to engage in their studies. He has a growing interest in the security and application of 5G wireless technologies. He has acted as a reviewer for numerous conferences and journals and a reviewer for the HEA in funding bids for technology enhanced learning. He is a member of the British Computer Society.

ABIR J. HUSSAIN (Member, IEEE) received the Ph.D. degree from The University of Manchester (UMIST), U.K., in 2000.

Her Ph.D. thesis title Polynomial Neural Networks for Image and Signal Processing. She is currently a Professor in machine learning with the University of Sharjah, United Arab Emirates. She has published numerous refereed research papers in conferences and journals in the research areas of neural networks, signal prediction, telecommunication fraud detection, and image compression. Her research has been published in a number of high esteemed and high impact journals. She is also a Ph.D. Supervisor and an External Examiner for research degrees, including Ph.D. and M.Phil. She is one of the initiators and chairs of the Development in e-Systems Engineering (DeSE) series, most notably illustrated by the IEEE technically sponsored DeSE International Conference Series. Her research interests include machine learning algorithms and their applications to medical, image and signal processing, and data analysis.